

Electrical-conductivity calculation in *ab initio* simulations of metals: Application to liquid sodium

Pier Luigi Silvestrelli

Max-Planck-Institut für Festkörperforschung, Heisenbergstrasse 1, 70569 Stuttgart, Germany

Ali Alavi

*Atomistic Simulation Group, School of Mathematics and Physics, The Queen's University, Belfast BT7 1NN, Northern Ireland,
United Kingdom*

Michele Parrinello

*Max-Planck-Institut für Festkörperforschung, Heisenbergstrasse 1, 70569 Stuttgart, Germany
(Received 16 December 1996)*

We describe a calculation of the electrical conductivity in *ab initio* simulations of liquid sodium, using the Kubo-Greenwood formula for the optical conductivity and the molecular-dynamics scheme based on finite-temperature density functional theory. The effect of different Brillouin-zone samplings and that of the finite size of the system have been extensively studied at different temperatures. Close to the melting point, even with an adequate sampling of the Brillouin zone, our results exhibit a large discrepancy between theory and experiment. This is much reduced at higher temperatures. The possible reasons for this behavior are discussed. [S0163-1829(97)00723-6]

I. INTRODUCTION

As the temperature of a metal approaches the melting point T_m , its electrical resistivity ρ rises approximately linearly; at T_m , ρ increases abruptly, and then continues to rise approximately linearly in the liquid state.¹ Many calculations of ρ and its temperature dependence have been reported, particularly in alkali metals.²⁻⁷ In all these calculations the Ziman approach has been used.

The theory of Ziman⁸ is based on a quasi-free-electron approximation and makes use of the Boltzmann approach to transport. The crucial ingredients of the theory are the static structure factor $S(k)$ and the pseudopotentials. On the whole the Ziman method has been rather successful in describing the conductivity of many liquid metals close to the melting point. However, recent attempts⁷ at calculating the high-temperature conductivity proved partially unsuccessful. The results were particularly unsatisfactory for Na, Al, and Pb. Since both pseudopotentials and structure factor are accurately known for these elements, the discrepancy with the experimental values can be attributed to the use of the weak-scattering approximation, which becomes more and more invalid as the temperature is raised. The limitation of the Ziman formula can in principle be circumvented by present day developments of *ab initio* molecular dynamics (MD).⁹ In this approach the interactions are computed from first-principles calculations performed on the fly as the simulation proceeds. This gives access to the electronic excitation spectrum. Using this information the electrical conductivity can be calculated from the Kubo-Greenwood formula.¹⁰ This in principle straightforward procedure allows one to transcend the weak-scattering limit of the Ziman formula.

The *ab initio* simulation of metals poses a variety of technical problems for which different solutions have been proposed.¹¹ Here we shall follow the approach of Alavi

et al.,^{12,13} which is based on a new formulation of the finite-temperature Mermin density functional theory (DFT).¹⁴ We will examine various problems connected with the use of finite simulation cell and make a complete analysis of the k -point sampling of the Brillouin zone (BZ). As is well known, in small cells a poor k -point sampling induces the appearance of artificial energy gaps, as large as 1 eV, close to the Fermi level. Since the electrical conductivity crucially depends on the density of states at the Fermi surface, this point has to be carefully examined. By performing simulations, at various temperatures, with different k -point grids and different sizes of the supercell, we show that a suitable choice of the k -point sampling can significantly reduce the computational cost. In fact reasonable estimates of the electrical conductivity can be obtained using relatively small supercells. Finally, we compare our results with the experimental data and we comment on the discrepancy observed between simulation and experiment.

II. COMPUTATIONAL SCHEME

Simulations have been performed using the method of *ab initio* MD based on the finite-temperature density functional theory of Alavi *et al.*^{12,13,15} This technique is particularly suitable for studying electronic properties of metallic systems since a self-consistent electronic-structure calculation is performed at each MD step and the effect of thermal electronic excitations is consistently incorporated using fractionally occupied states.

Most of the simulations have been carried out in a periodically repeated simple cubic box containing $N=90$ sodium atoms. With this value of N , using the Γ point only to sample the BZ, the Fermi level is located in the middle of a quasidegenerate set of energy levels. Therefore no large, unphysical energy gap is present between conduction and valence bands.

TABLE I. Equilibrium distance d and vibrational frequency ω of Na_2 , as obtained by computer simulation, using the Topp-Hopfield pseudopotential, and the plane-wave energy cutoff of 5 and 8 Ry, respectively. Comparison is made with the results of other *ab initio* simulations (based on different pseudopotentials) and the experiment.

	d (a.u.)	ω (cm^{-1})
Topp-Hopfield (5 Ry)	5.87	145
Topp-Hopfield (8 Ry)	5.87	146
Reference 19	5.48	173
Reference 20	5.56	163
Experiment ^a	5.82	159

^aReference 21.

The size of the cubic box has been varied to reproduce the experimental densities¹⁶ of liquid sodium at five different temperatures above the melting point ($T_m = 371$ K), namely, $T = 400, 550, 700, 850,$ and 1000 K. finite-size effects have been studied by At $T = 400$ and 700 K finite-size effects have been studied by performing simulations with an increasing number of sodium atoms. Again, the values of N ($N = 46, 60, 90, 138, 206$) have been chosen in such a way that, using the Γ -point sampling, the Fermi level is placed in the middle of a quasidegenerate set of energy levels. The interaction between ions and valence electrons has been modeled using the Topp-Hopfield¹⁷ (TH) pseudopotential

$$V_{\text{TH}}(r) = \begin{cases} V_0 \cos(ar) + b, & r \leq r_c \\ -1/r, & r > r_c, \end{cases} \quad (1)$$

where the numerical values (in a.u.) of the parameters are $V_0 = 0.179$, $a = 1.224$, $b = -0.179$, and $r_c = 3.0$. $V_{\text{TH}}(r)$ is a local potential, which correctly reproduces the ground state and the lowest excitation energy of the isolated sodium atom in a Hartree-Fock calculation. The pseudopotential of Eq. (1) is not state of the art, however, it has been successfully used^{17,18} to study structural and dynamical properties of solid sodium. Furthermore it has the advantage of being a very smooth potential, so that the electronic orbitals can be expanded in plane waves using a relatively low energy cutoff of ~ 5 Ry. This feature allowed us to simulate relatively large systems at a reduced computer cost. Preliminary tests have been performed to check the adequacy of the chosen pseudopotential. In Table I we have reported the equilibrium distance and vibrational frequency of the Na_2 molecule, computed using the Topp-Hopfield pseudopotential. As can be seen, by increasing the energy cutoff from 5 to 8 Ry the results have not appreciably changed. Moreover the comparison with other pseudopotential calculations and experiment appears to be satisfactory.

For a given configuration of ions, the electronic density $n(\mathbf{r})$ has been computed by minimizing the free energy functional F of the electron gas. This is defined as

$$F = \Omega + \mu N_e + E_{II}, \quad (2)$$

where

$$\Omega[n(\mathbf{r})] = -\frac{2}{\beta} \ln \det(1 + e^{-\beta(\mathcal{H} - \mu)}) - \int d\mathbf{r} n(\mathbf{r}) \left(\frac{\phi(\mathbf{r})}{2} + \frac{\delta\Omega_{\text{xc}}}{\delta n(\mathbf{r})} \right) + \Omega_{\text{xc}}, \quad (3)$$

where $\beta = 1/(k_B T_{\text{el}})$ is the inverse electronic temperature, μ is the chemical potential, N_e is the total number of valence electrons, $\mathcal{H} = -(1/2)\nabla^2 + V(\mathbf{r})$ is the one-electron Hamiltonian with the effective potential $V(\mathbf{r}) = \sum_I V_{eI}(\mathbf{r} - R_I) + \phi(\mathbf{r}) + \delta\Omega_{\text{xc}}/\delta n(\mathbf{r})$, $\phi(\mathbf{r})$ is the Hartree potential of an electron gas of density $n(\mathbf{r})$, Ω_{xc} the exchange-correlation energy in the local-density approximation (LDA), and E_{II} the classical Coulomb energy of the ions. The functional Ω_{xc} is approximated by its $T_{\text{el}} = 0$ expression, since its finite-temperature corrections are negligible²² at the temperatures and the electronic densities of our system. F reproduces the exact finite-temperature density of the Mermin functional¹⁴ and was self-consistently optimized, for each ionic configuration, using as the electronic temperature the average ionic temperature. Efficient diagonalization of the one-electron Hamiltonian has been performed by means of a variant²³ of the Lanczos algorithm, which allows optimal use of a good guess of the initial wave function. The electronic density is expressed in terms of the single-particle orbitals

$$n(\mathbf{r}) = \sum_i f_i |\psi_i(\mathbf{r})|^2, \quad (4)$$

where f_i are the Fermi-Dirac occupation numbers, $f_i = (e^{\beta(E_i - \mu)} + 1)^{-1}$, and the ionic forces are calculated using the Hellmann-Feynman theorem. The ionic degrees of freedom have been integrated using a time step of 50 a.u. (~ 1.2 fs). The starting potential for each time step has been calculated (see Appendix) from the converged electronic charge density of the previous time step plus the difference between a superposition of atomiclike charge densities at the current and previous times. This procedure has significantly reduced (typically from 5–10 to 2–3) the number of iterations required to achieve self-consistency. In the first part of each simulation the system has been equilibrated, for ~ 1 ps, at a given average ionic temperature, starting from a disordered initial configuration. Then a production run of ~ 1 ps has been performed in which structural and electronic properties of the system have been computed. The Γ point only was used to sample the BZ of the MD supercell. However, for a selected set of ionic configurations, the one-electron Hamiltonian has been also diagonalized using different, more thorough, k -point samplings, according to the prescription of Monkhorst and Pack.²⁴ In these cases we have not performed a full self-consistent optimization, but we have used the converged electronic density obtained by the Γ -point sampling. This is a good approximation, as we have explicitly checked for some ionic configurations: the effect on the free energy is negligible (the relative error being of the order of $\sim 10^{-4}$) and the relative error in the electrical conductivity is $\sim 1\%$, which is a value smaller than the typical statistical errors of this quantity.

As in other *ab initio* simulations^{13,25} we have computed the electrical conductivity σ by extrapolating to zero fre-

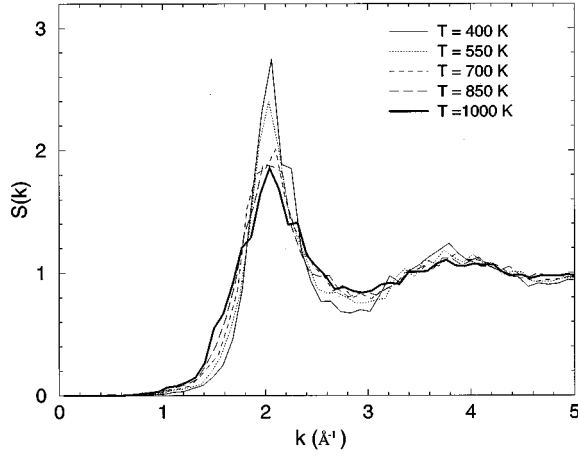


FIG. 1. Static structure factor $S(k)$ of liquid sodium ($N=90$) at different temperatures. The curves have been obtained by averaging over the configurations of the MD simulation.

quency the results obtained by the Kubo-Greenwood formula¹⁰ for the optical conductivity:

$$\sigma = \sigma(0) = \lim_{\omega \rightarrow 0} \sigma(\omega), \quad (5)$$

with $\sigma(\omega)$ computed as a configurational average of

$$\begin{aligned} \sigma(\omega, R_I) = & \frac{2\pi e^2}{3m^2\omega} \frac{1}{V_b} \sum_{i,j} (f_i - f_j) |\langle \psi_i | \hat{p} | \psi_j \rangle|^2 \\ & \times \delta(E_j - E_i - \hbar\omega), \end{aligned} \quad (6)$$

where e and m are the electronic charge and mass, $V_b = L^3$ is the simulation box volume, \hat{p} is the momentum operator and ψ_i , E_i , are the electronic DFT eigenstates and eigenvalues, calculated for the ionic configuration $\{R_I\}$, at a single k point (for instance, the Γ point) of the BZ. The generalization of Eq. (6) to more than one k vector is straightforward:

$$\sigma(\omega, R_I) = \sum_{\mathbf{k}} \sigma(\omega, R_I, \mathbf{k}) \cdot W(\mathbf{k}), \quad (7)$$

where $\sigma(\omega, R_I, \mathbf{k})$ is defined by Eq. (6), with the eigenstates and the eigenvalues computed at \mathbf{k} , and $W(\mathbf{k})$ is the weight of the point \mathbf{k} . Of course, the use of the single-particle DFT states and eigenvalues, instead of the true many-body eigenfunctions and eigenvalues, introduces an approximation in the calculation of σ . Due to the finite-size discretization of the eigenvalue spectrum, in practical applications $\sigma(\omega, R_I)$ is computed for a finite set of frequencies $(\omega_1, \omega_2, \dots, \omega_l, \dots)$ by averaging over a small frequency range $\Delta\omega$:

$$\sigma(\omega_l, R_I) \approx \frac{1}{\Delta\omega} \int_{\omega_l - \Delta\omega/2}^{\omega_l + \Delta\omega/2} \sigma(\omega, R_I) d\omega. \quad (8)$$

The value of $\Delta\omega$ must be carefully chosen. In fact it has to be large enough to assure that a sufficient number of electronic levels contribute, and, at the same time, small enough to allow a good resolution. We have found that $\Delta\omega = 0.05$ eV is adequate for our system. Since our computed $\sigma(\omega)$ curves are smooth functions, we have estimated the dc con-

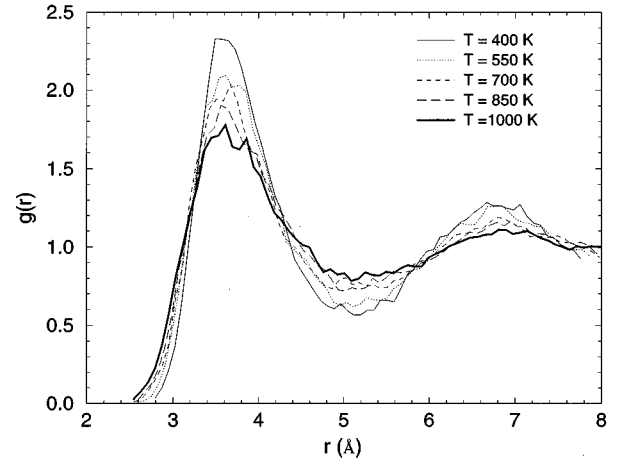


FIG. 2. Pair correlation function $g(r)$ of liquid sodium ($N=90$) at different temperatures. The curves have been obtained by averaging over the configurations of the MD simulation.

ductivity by a simple linear extrapolation, using the averaged values of $\sigma(\omega)$ calculated at the two lowest frequencies. Notice that $\sigma(\omega)$ must obey a sum rule¹⁰ that can be easily obtained as a generalization of the sum rule of the oscillator strength:

$$S = \frac{2mV_b}{\pi e^2 N_e} \int_0^\infty d\omega \sigma(\omega) = 1. \quad (9)$$

In actual calculations S is expected to be smaller than 1, since only a finite, limited number of excited states can be taken into account in the evaluation of Eq. (6).

III. RESULTS AND DISCUSSION

In Figs. 1 and 2 we have plotted the static structure factor $S(k)$ and the pair correlation function $g(r)$ of liquid sodium, at different temperatures. The curves have been obtained by averaging over the ionic configurations of the MD simulations, performed with $N=90$. The effect of increasing the

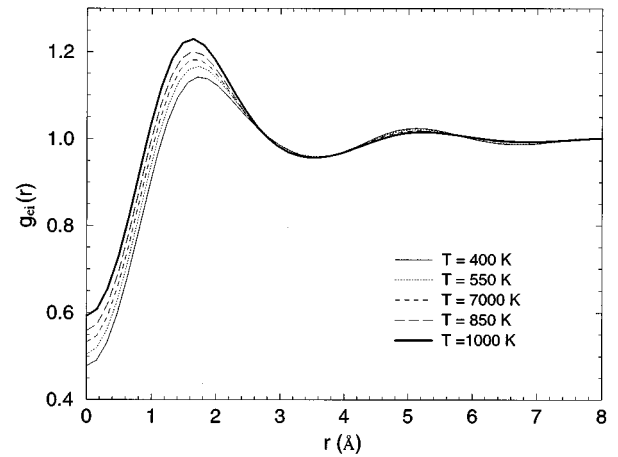


FIG. 3. Electron-ion pair correlation function $g_{ei}(r)$ of liquid sodium ($N=90$) at different temperatures. The curves have been obtained by averaging over the configurations of the MD simulation.

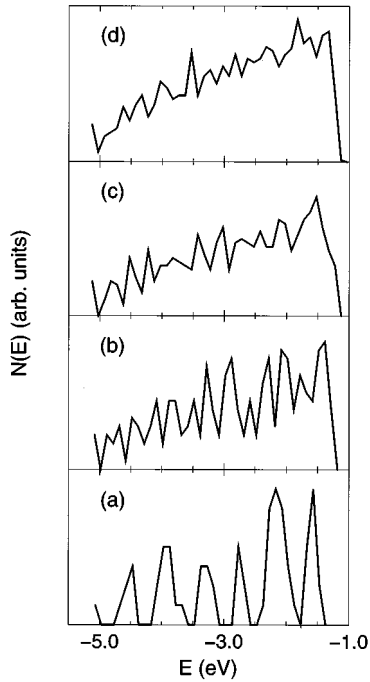


FIG. 4. Electronic density of states $N(E)$ of a single MD configuration of liquid sodium ($N=90$) at 700 K, obtained by using increasingly large sets of k vectors to sample the BZ: (a) Γ point, (b) 8 k points, (c) 18 k points, (d) 48 k points. The curves have been averaged over energy intervals of width 0.1 eV.

temperature is evident. The peaks become flatter and broader. In particular the height of the first peak decreases gradually whereas its width increases on raising the temperature. Our computed $S(k)$ and $g(r)$ functions are in good agreement with the results obtained by experiments²⁶ and theoretical models.⁷ The success of this and previous *ab initio* simulations²⁷ of liquid sodium can be taken as an indication of the adequacy of the Γ -point sampling for the evaluation of the structural properties. This conclusion is strengthened by the observed insensitivity of the $g(r)$ to the cell size.

The same is true for the electronic density, as we have already pointed out in Sec. II. In Fig. 3 we have plotted the electron-ion pair correlation function $g_{ei}(r)$ of liquid sodium ($N=90$) at different temperatures. This function describes the correlation between the local density of the valence electrons and the local density of the ions. As in Ref. 28 we have computed $g_{ei}(r)$ according to

$$g_{ei}(r) = \frac{1}{4\pi r^2 n_0 N} \left\langle \sum_I^N \int d\mathbf{r}' n(\mathbf{r}') \delta(|\mathbf{r}' - \mathbf{R}_I| - r) \right\rangle, \quad (10)$$

where n_0 is the averaged density of electrons and the angular brackets indicate temporal average. Our $g_{ei}(r)$ curve, computed at 400 K, is in good agreement with the same function calculated, at 373 K, by Ishitobi and Chihara,²⁹ using the hypernetted-chain approximation. As can be seen, the probability that the valence electronic charge is close to a given ion increases as the temperature rises. This reflects an increased electron charge localization. It is very hard to assess whether this indicates that the system is approaching the

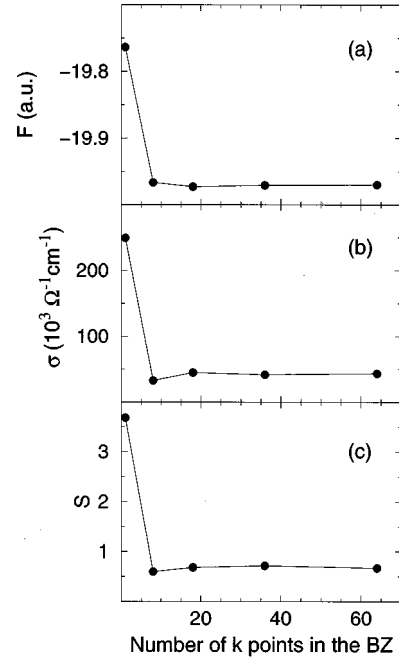


FIG. 5. Convergence of electronic properties of liquid sodium ($N=90$), for a single MD configuration at 400 K, as a function of the number of k points used in the sampling of the BZ: (a) free energy F , (b) dc conductivity σ , (c) $S = 2mV_b / (\pi e^2 N_e) \int_0^\infty d\omega \sigma(\omega)$. Symbols indicate computed values, while the lines are just a guide for the eye.

metal-insulator transition since LDA has well-known problems in describing such a transition, characterized by a complicated interplay between disorder and electron interaction effects.³⁰

While, at $N=90$, the Γ -point sampling appears to be adequate in describing the structural properties and the valence charge distribution of the system, it is significantly less accurate in reproducing the electronic density of states (EDOS) and in the computation of the electrical conductivity σ . These conclusions will be made evident by the following detailed analysis.

In Fig. 4 we have reported the EDOS corresponding to a single MD configuration of liquid sodium ($N=90$) at 700 K, that is just in the middle of the range of temperatures we have considered. The EDOS actually displayed have been averaged over energy intervals of width 0.1 eV, and they have been obtained using different k -point samplings. As can be seen, the Γ -point sampling gives a poor representation of the EDOS, which, in our system, is expected to be nearly free-electron-like. The situation clearly improves by increasing the number of k points that are used. In particular, a k -point sampling consisting of the 8 points ($\pm 1/4, \pm 1/4, \pm 1/4$) π/L turns out to be already sufficient to obtain a reasonable EDOS behavior. The same is true for the MD configurations sampled at the other temperatures we have considered.

A similar conclusion can be drawn by considering the calculation of the electrical conductivity, for which a more quantitative analysis can be performed. In Fig. 5 we report the behavior of the free energy F , the dc conductivity σ , and the value of S , as a function of the number of k vectors used

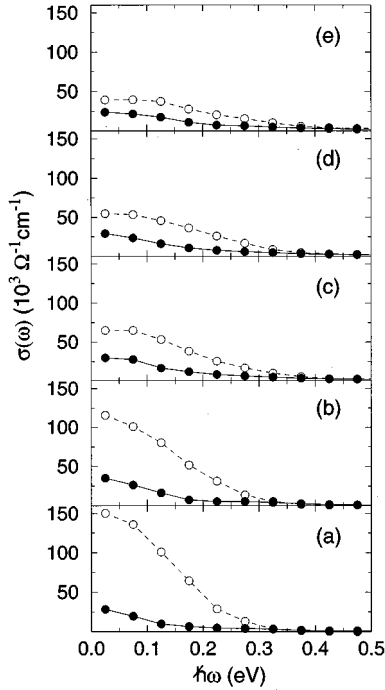


FIG. 6. Optical conductivity $\sigma(\omega)$ of liquid sodium ($N=90$), computed at different temperatures, averaging over 10 uncorrelated configurations of the MD simulation: (a) 400 K, (b) 550 K, (c) 700 K, (d) 850 K, (e) 1000 K. The open circles have been obtained using the Γ -point sampling, while the full circles are the results computed by the 8- k -vector sampling. The solid and dashed lines are just a guide for the eye.

in the sampling of the BZ. In this case we have considered a single MD configuration at 400 K, since we expect that, at low temperature, the convergence of the electronic properties is slower than at high temperature. In fact, by increasing the temperature, the resulting broadening of the Fermi function lowers the energy resolution needed and therefore a coarser k -point sampling is sufficient. As can be seen, 8 k vectors give reasonably converged results. We also note that, using the Γ -point only sampling, we obtain $S > 1$. Such a violation of the sum rule is not a result of the numerical approximation used but is instead a consequence of the poor k -point sampling. For larger k -point samplings $S = 1$ is not exactly satisfied but it is $S < 1$ that is to be ascribed, as discussed earlier, to a truncated summation over the excited states.

In Fig. 6 the optical conductivity curves, obtained at different temperatures, averaging over 10 uncorrelated ionic configurations of the MD simulation, have been plotted. The statistical error bars have been omitted for clarity, typical relative errors being of the order of 5–10%. Table II reports the corresponding values of S . As can be seen there is a remarkable difference between the results obtained using the Γ point and the 8- k -vector sampling. As expected, the discrepancy reduces by increasing the temperature, however, even at 1000 K, S is larger than 1 with the Γ -point sampling. In nearly-free-electron metals the optical conductivity should exhibit a Drude-like behavior. Therefore we have tried to fit our computed $\sigma(\omega)$ data of Fig. 6 to the Drude function

$$\sigma(\omega) = \frac{N_e e^2 \tau}{\Omega m} \frac{1}{1 + \omega^2 \tau^2}. \quad (11)$$

TABLE II. Values of $S = 2mV_b / (\pi e^2 N_e) \int_0^\infty d\omega \sigma(\omega)$, averaged over 10 uncorrelated MD configurations of liquid sodium ($N=90$), at different temperatures, obtained using the Γ -point sampling, $S(\Gamma)$, and the 8- k -point sampling, $S(8k)$. Statistical errors, in the last digit, are given in parentheses. $\tau(8k)$ are the relaxation times calculated by fitting Drude curves to the $\sigma(\omega)$ data (see Fig. 6), obtained by the 8- k -point sampling.

T (K)	$S(\Gamma)$	$S(8k)$	$\tau(8k)$ (10^{-15} sec)
400	3.55 (8)	0.59 (2)	7.0
550	2.92 (9)	0.82 (3)	6.9
700	2.29 (9)	0.91 (3)	5.1
850	2.12 (5)	0.91 (1)	4.9
1000	1.86 (6)	0.92 (1)	4.5

We have found that the curves obtained using the 8- k -vector sampling are reproduced by a Drude function much better than those computed with the Γ -point sampling. This can represent a further indication that the Γ -point approximation is not adequate to describe the electronic properties of the system. In Table II the estimated values of the Drude relaxation time τ are shown. As expected τ decreases by increasing the temperature.

Finite-size effects have been studied by performing simulations of liquid sodium, at $T=400$ and 700 K, with different values of N , in the range 46–206, using the Γ -point sampling. In all the cases the Fermi level was located in the middle of a quasidegenerate set of levels. In Figs. 7 and 8 we have reported the behavior of S and σ as a function of N , for $T=400$ and 700 K, respectively. It is evident that, by increasing the size of the system, the convergence of these quantities is quite slow, particularly at $T=400$ K. In fact, in this case, even using a large supercell containing 206 atoms, the conductivity value appears to be far from conver-

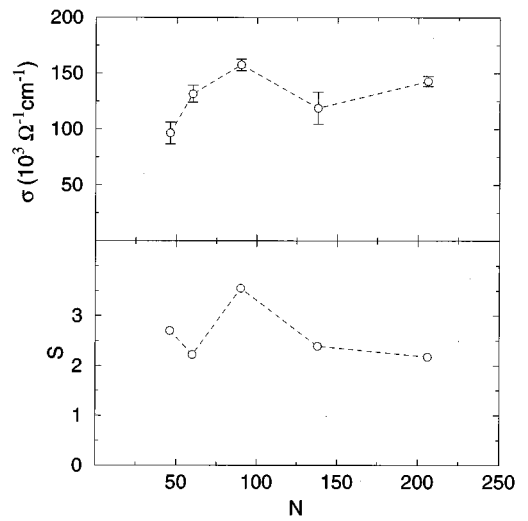


FIG. 7. Finite-size effects in liquid sodium. Convergence of σ (upper panel) and S (lower panel), at 400 K, as a function of N , the number of sodium atoms used in the simulation. The BZ has been sampled using the Γ point only. Circles indicate computed values (averaging over 10 uncorrelated configurations of the MD simulation), while the lines are just a guide for the eye. Statistical errors of S are of the same size as the symbols.

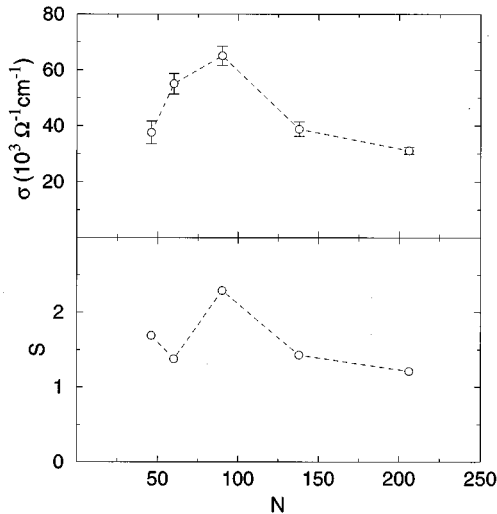


FIG. 8. Finite-size effects in liquid sodium. Convergence of σ (upper panel) and S (lower panel), at 700 K, as a function of N , the number of sodium atoms used in the simulation. The BZ has been sampled using the Γ point only. Circles indicate computed values (averaging over 10 uncorrelated configurations of the MD simulation), while the lines are just a guide for the eye. Statistical errors of S are of the same size of the symbols.

gence, as indicated by the fact that the sum rule is not satisfied. Instead, at $T=700$ K, with $N=206$ the value of S is not much larger than 1, suggesting that σ is approaching the converged value. Therefore we can conclude that, using the Γ -point sampling, a simulation box containing at least 200 sodium atoms is necessary in order to obtain reasonably converged conductivity values, at $T=700$ K. For lower temperatures our results indicate that a considerably larger supercell is required. Notice that, in the case of $T=700$ K, our σ computed at $N=206$ is very close to the value obtained at $N=90$, using the 8- k -vector sampling. This interesting result is confirmed by analysis of Fig. 9, where we compare the

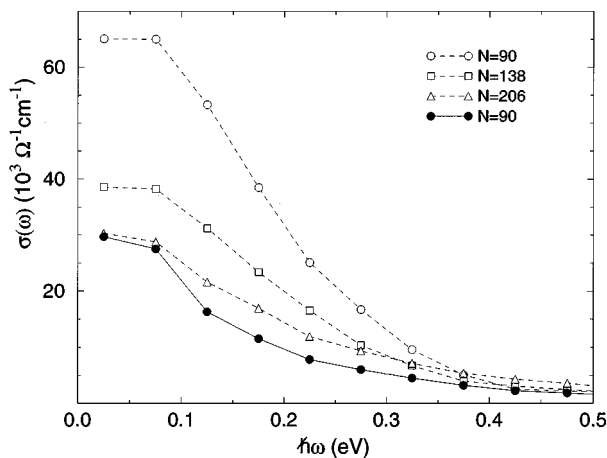


FIG. 9. Optical conductivity $\sigma(\omega)$ of liquid sodium, at 700 K, using the Γ -point sampling of the BZ with different values of N (open symbols), and the 8- k -vector sampling with $N=90$ (full circles). Symbols indicate computed values (averaging over 10 uncorrelated configurations of the MD simulation), while the lines are just a guide for the eye.

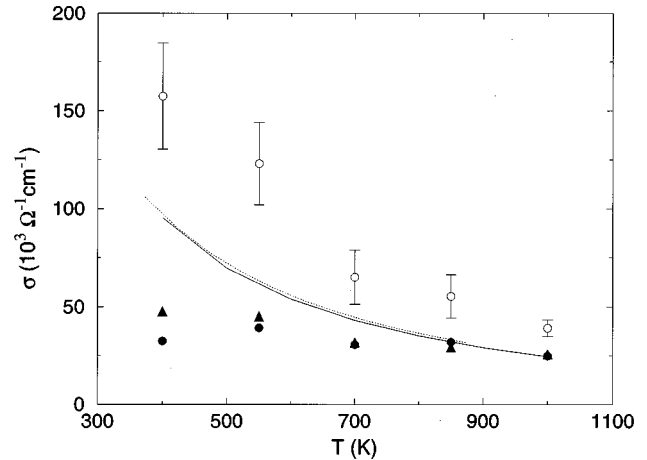


FIG. 10. Electrical conductivity σ of liquid sodium ($N=90$) as a function of the temperature. The open circles have been obtained using the Γ -point sampling, while the full symbols are the results computed by the 8- k -vector sampling. In this last case σ has been obtained both by extrapolating $\sigma(\omega)$ to zero frequency (circles), and using the formula $\sigma=N_e e^2 \tau / \Omega m$ with τ estimated by fitting $\sigma(\omega)$ to the Drude function (triangles). The solid and dotted lines connect points taken from two sets of experimental data (Ref. 31).

optical conductivity functions $\sigma(\omega)$ computed at $N=90$, $N=138$, and $N=206$, using the Γ -point sampling, with the same quantity obtained at $N=90$, using the 8- k -vector sampling. As can be seen, the curve computed at $N=206$ is very similar to that calculated at $N=90$ with the 8- k -vector sampling. This turns out to be particularly true at the lowest frequencies, that is, just in the region that is more relevant to extrapolate the value of σ . Since the computational cost of our *ab initio* simulations scales approximately as $N^3 \times N_k$, where N_k is the number of the k vectors that are taken into account in the actual calculation ($N_k=4$ for the 8- k -vector sampling, due to symmetry considerations), it is clear that, also in our disordered system, a careful choice of the k -point sampling can be very effective in decreasing the computational effort that is required to estimate the electrical conductivity.

Finally, in Fig. 10, we have plotted our calculated electrical conductivity σ as a function of the temperature. In the case of the 8- k -vector sampling we have computed σ in two ways, using the standard procedure of extrapolating $\sigma(\omega)$ to zero frequency, and by means of the Drude formula, which allows us to obtain σ from the estimate of the relaxation time τ , $\sigma=N_e e^2 \tau / \Omega m$. The difference between the values of σ computed using the two methods can be taken as an estimate of the uncertainty inherent in the extrapolation of $\sigma(\omega)$ to zero frequency. As can be seen the difference between the two estimates is very small except in the case of $T=400$ K. By comparison with the experimental curves one can observe that all the values computed using the Γ -point sampling are considerably higher than the corresponding experimental data. With the 8- k -vector sampling our results are compatible with the experiment at $T=850$ and 1000 K, however, there is a clear disagreement at lower temperatures. Hence the temperature dependence of the electrical resistivity is not well reproduced. This unsatisfactory result does not appear to be related to a poor sampling of the BZ or to

finite-size effects. In fact, as we have already discussed, using more than 8 k points does not significantly affect the results (see Fig. 5). Moreover, our estimated value of σ is clearly not compatible with the experiment even at $T=700$ K and $N=206$, namely, in a situation in which we can assume (see Fig. 8) that the computed conductivity is reasonably converged with respect to the size of the simulation cell.

In principle, the observed discrepancy could be attributed to the chosen electron-ion pseudopotential. In order to check this possibility, we have performed some tests, for a few selected MD configurations at 400 K, with different, norm-conserving, sodium pseudopotentials.³² However, the agreement with experiment has not substantially improved. We have even considered the possibility that nonlinear core corrections^{20,33} might play a role. Unfortunately explicit calculations have shown this not to be the case.

Hence what we are left with are the approximations involved in the calculation of σ by means of the Kubo-Greenwood formula, particularly the use of DFT eigenstates and eigenvalues in place of the true many-body quantities, and the fact that, as the temperature decreases and the system becomes more and more free-electron-like, the procedure of extrapolating $\sigma(\omega)$ to zero frequency is more delicate and less reliable. Moreover another finite-size effect might be responsible for the poor performance of the theory. In fact in a small system large-wavelength ionic fluctuations are suppressed by the periodic boundary conditions, and therefore the associated contribution to the conductivity is neglected.

IV. CONCLUSIONS

In conclusion, we have presented a calculation of structural and electronic properties of liquid sodium using finite-temperature, *ab initio* MD simulation. A detailed analysis has shown that the Γ -point approximation, although reliable to compute structural properties and ‘‘integral’’ quantities, such as the free energy, the electron density, and the Hellmann-Feynman forces, is much less accurate in reproducing other electronic properties, particularly the electrical conductivity. In fact reasonably converged results can be obtained using large systems only. As expected, the minimum size of the simulation cell decreases as the temperature increases, however, even at $T=700$ K, a system containing at least 200 atoms is required if the Γ -point approximation is used. In contrast, by performing simulations with 90 sodium atoms, the use of a relatively small set of k vectors, consisting of 8 points, appears to be sufficient to obtain a reasonable sampling of the BZ and to substantially reduce finite-size effects. Therefore, as to be expected, a careful choice of the k -point sampling can considerably improve the efficiency of *ab initio* simulations of liquid metals. By studying the behavior of the electrical conductivity, as a function of the temperature, we find that, even using a proper k -point sampling, our results are in agreement with the experimental data for temperatures higher than 700 K only. This effect is probably related to the approximations introduced in the actual calculation of the optical conductivity and in the extrapolation of this quantity to zero frequency.

ACKNOWLEDGMENTS

Part of this work was supported by the Nederlandse Organisatie voor Wetenschappelijk Onderzoek (NWO).

APPENDIX

In our MD simulation the self-consistent optimization of the free-energy functional F has been efficiently performed using the following scheme.

If one assumes that a superposition of atomiclike charge densities is a good approximation of the actual charge distribution $n(\mathbf{r})$, then, at the simulation time t , one can write

$$n_t(\mathbf{r}) \approx \tilde{n}_t(\mathbf{r}) = \sum_{\mathbf{I}} n_{\text{at}}[\mathbf{r} - \mathbf{R}_{\mathbf{I}}(t)] = \sum_{\mathbf{G}} [n_{\text{at}}(\mathbf{G}) S_t(-\mathbf{G})] e^{i\mathbf{G}\mathbf{r}}, \quad (\text{A1})$$

where $n_{\text{at}}(\mathbf{r})$ and $n_{\text{at}}(\mathbf{G})$ are the atomic charge distribution and its Fourier transform, respectively, and $S_t(\mathbf{G})$ is the atomic structure factor defined as $S_t(\mathbf{G}) = \sum_{\mathbf{I}} e^{i\mathbf{G}\mathbf{R}_{\mathbf{I}}(t)}$. From Eq. (A1) one obtains

$$n_t(\mathbf{G}) \approx \tilde{n}_t(\mathbf{G}) = n_{\text{at}}(\mathbf{G}) S_t(-\mathbf{G}) \quad (\text{A2})$$

and

$$n_{\text{at}}(\mathbf{G}) \approx n_t(\mathbf{G}) / S_t(-\mathbf{G}). \quad (\text{A3})$$

The basic idea is to use, as the input charge density at time $t + \Delta t$, the converged, output density at time t plus the difference between the superposition of the atomic charge densities at time $t + \Delta t$ and t , respectively:

$$n_{t+\Delta t}^{\text{inp}}(\mathbf{r}) = n_t^{\text{out}}(\mathbf{r}) + [\tilde{n}_{t+\Delta t}(\mathbf{r}) - \tilde{n}_t(\mathbf{r})]. \quad (\text{A4})$$

Hence, by using Eq. (A2) and Fourier transforming, we have

$$n_{t+\Delta t}^{\text{inp}}(\mathbf{G}) = n_t^{\text{out}}(\mathbf{G}) + n_{\text{at}}(\mathbf{G}) [S_{t+\Delta t}(-\mathbf{G}) - S_t(-\mathbf{G})]. \quad (\text{A5})$$

Finally, we can write

$$\begin{aligned} n_{t+\Delta t}^{\text{inp}}(\mathbf{G}) &= n_t^{\text{out}}(\mathbf{G}) + n_t^{\text{out}}(\mathbf{G}) \left[\frac{S_{t+\Delta t}(-\mathbf{G})}{S_t(-\mathbf{G})} - 1 \right] \\ &= n_t^{\text{out}}(\mathbf{G}) \frac{S_{t+\Delta t}(-\mathbf{G})}{S_t(-\mathbf{G})}, \end{aligned} \quad (\text{A6})$$

where Eq. (A3) has been used.

We have found that this scheme significantly improves the efficiency of the self-consistent cycle. Typically only 2 or 3 iterations were sufficient to achieve self-consistency in place of the 5–10 iterations required by the standard procedure in which $n_{t+\Delta t}^{\text{inp}}(\mathbf{r}) = n_t^{\text{out}}(\mathbf{r})$. A similar technique has been also applied to simulations of liquid sodium by Bylander and Kleinman.²⁷

- ¹See, for instance, V. A. Alekseev and I. T. Iakubov, *Handbook of Thermodynamic and Transport Properties of Alkali Metals*, edited by R. W. Ohse (Blackwell Scientific, Oxford, 1985), Chap. 7.1.
- ²M. P. Greene and W. Kohn, *Phys. Rev.* **137**, A513 (1965).
- ³N. W. Ashcroft and J. Lekner, *Phys. Rev.* **145**, 83 (1966).
- ⁴J. F. Devlin and W. van der Lugt, *Phys. Rev. B* **6**, 4462 (1972).
- ⁵D. J. Stevenson and N. W. Ashcroft, *Phys. Rev. A* **9**, 782 (1974).
- ⁶H. Minoo, C. Deutsch, and J. P. Hansen, *J. Phys. (Paris) Lett.* **38**, L191 (1977).
- ⁷S. Sinha, P. L. Srivastava, and R. N. Singh, *J. Phys. Condens. Matter* **1**, 1695 (1989).
- ⁸J. M. Ziman, *Philos. Mag.* **6**, 1013 (1961).
- ⁹R. Car and M. Parrinello, *Phys. Rev. Lett.* **55**, 2471 (1985).
- ¹⁰R. Kubo, *J. Phys. Soc. Jpn.* **12**, 570 (1957); D. A. Greenwood, *Proc. Phys. Soc.*, **71**, 585 (1958).
- ¹¹C.-L. Fu and K.-M. Ho, *Phys. Rev. B* **28**, 5480 (1983); C. Woodward, B. I. Min, R. Benedek, and J. Garner, *ibid.* **39**, 4853 (1989); M. Methfessel and A. T. Paxton, *ibid.* **40**, 3616 (1989); G. W. Fernando, G.-X. Qian, M. Weinert, and J. W. Davenport, *ibid.* **40**, 7985 (1989); P. E. Blöchl and M. Parrinello, *ibid.* **45**, 9413 (1992); R. M. Wentzcovitch, J. L. Martins, and P. B. Allen, *ibid.* **45**, 11 372 (1992); M. P. Grumbach, D. Hohl, R. M. Martin, and R. Car, *J. Phys. Condens. Matter* **6**, 1999 (1994); S. de Gironcoli, *ibid.* **51**, 6773 (1995); G. Kresse and J. Furthmüller, *ibid.* **54**, 11 169 (1996); A. De Vita, N. Marzari, M. C. Payne, M. J. Gillan, and V. Heine (unpublished).
- ¹²A. Alavi, J. Kohanoff, M. Parrinello, and D. Frenkel, *Phys. Rev. Lett.* **73**, 2599 (1994).
- ¹³P. L. Silvestrelli, A. Alavi, M. Parrinello, and D. Frenkel, *Europhys. Lett.* **33**, 551 (1996); *Phys. Rev. B* **53**, 12 750 (1996).
- ¹⁴N. D. Mermin, *Phys. Rev.* **137**, A1441 (1965).
- ¹⁵We have used the k -point sampling version of the finite temperature *ab initio* MD code of A. Alavi and T. Deutsch, built from the code CPMD, version 3.0, developed by J. Hutter, P. Ballone, M. Bernasconi, P. Focher, E. Fois, S. Goedecker, M. Parrinello, M. Tuckerman, at MPI für Festkörperforschung and IBM Research (1990–1996).
- ¹⁶N. B. Vargaftik, V. F. Kozhevnikov, and V. A. Alekseev, *Handbook of Thermodynamic and Transport Properties of Alkali Metals*, edited by R. W. Ohse (Blackwell Scientific, Oxford, 1985), Chap. 6.3.4.
- ¹⁷W. C. Topp and J. J. Hopfield, *Phys. Rev. B* **7**, 1295 (1973).
- ¹⁸M. Pearson, E. Smargiassi, and P. A. Madden, *J. Phys. Condens. Matter* **5**, 3221 (1993); E. Smargiassi and P. A. Madden, *Phys. Rev. B* **49**, 5220 (1994).
- ¹⁹J. L. Martins, J. Buttet, and R. Car, *Phys. Rev. B* **31**, 1804 (1985).
- ²⁰U. Röthlisberger and W. Andreoni, *J. Chem. Phys.* **94**, 8129 (1991).
- ²¹K. P. Huber and G. Herzberg, *Constants of Diatomic Molecules* (Van Nostrand Reinhold, New York, 1979).
- ²²F. Perrot and M. W. C. Dharma-wardana, *Phys. Rev. A* **30**, 2619 (1984); D. G. Kanhere, P. V. Panat, A. K. Rajagopal, and J. Callaway, *ibid.* **33**, 490, (1986).
- ²³W. T. Pollard and R. A. Friesner, *J. Chem. Phys.* **99**, 6742 (1993).
- ²⁴H. J. Monkhorst and J. D. Pack, *Phys. Rev. B* **13**, 5188 (1976).
- ²⁵E. Fois, A. Selloni, and M. Parrinello, *Phys. Rev. B* **39**, 4812 (1989); G. Galli, R. Martin, R. Car, and M. Parrinello, *ibid.* **42**, 7470 (1990); I. Štich, R. Car, and M. Parrinello, *ibid.* **44**, 4262 (1991); **44**, 11 092 (1991).
- ²⁶Y. Waseda, *The Structure of Non-Crystalline Materials* (McGraw-Hill, New York, 1980).
- ²⁷D. M. Bylander and L. Kleinman, *Phys. Rev. B* **45**, 9663 (1992).
- ²⁸G. A. de Wijs, G. Pastore, A. Selloni, and W. van der Lugt, *Phys. Rev. Lett.* **75**, 4480 (1995).
- ²⁹M. Ishitobi and J. Chihara, *J. Phys. Condens. Matter* **4**, 3679 (1992).
- ³⁰D. E. Logan, I. J. Bush, and P. A. Madden, *Z. Phys. Chem.* **184**, 25 (1994).
- ³¹T. C. Chi, *J. Phys. Chem. Ref. Data* **8**, 339 (1979); J. F. Freedman and W. D. Robertson, *J. Chem. Phys.* **34**, 769 (1961).
- ³²G. B. Bachelet, D. R. Hamann, and M. Schlüter, *Phys. Rev. B* **26**, 4199 (1982); L. Kleinman and D. M. Bylander, *Phys. Rev. Lett.* **48**, 1425 (1982); N. Troullier and J. L. Martins, *Phys. Rev. B* **43**, 1993 (1991).
- ³³S. G. Louie, S. Froyen, and M. L. Cohen, *Phys. Rev. B* **26**, 1738 (1982).